



Variability of NmF2 and its correlation with solar and geomagnetic variations at an equatorial station in the African sector

Abdullahi Kikelomo Kazeem^{a*}, Adeniji Olayinka Olawepo^b & Akeem Babatunde Rabi^c

^aDepartment of Physics, Federal University of Technology, P M B 704, Akure, Ondo State, Nigeria

^bDepartment of Physics, University of Ilorin, P M B 1515, Ilorin, Kwara State, Nigeria

^cCentre for Atmospheric Research, National Space Research & Development Agency (NASRDA), Kogi State University Campus, Anyigba, Kogi State, Nigeria

Received: 16 June 2020; Accepted: 19 November 2020

This study focuses on the variability of NmF2 and the impact of the solar and geomagnetic activity on the variability of NmF2 over Ouagadougou, an equatorial ionisation anomaly station in the African sector. The daily hourly values of the critical frequency (f_oF2) covering two different solar cycles are used to study the variability of NmF2. The solar and geomagnetic data are used to examine their effect on the variability of NmF2. The results show that NmF2 displays obvious diurnal, seasonal and solar cycle effects. The semi-annual variation, winter and annual anomalies of NmF2 are clearly seen at all levels of solar activities. There is equinoctial asymmetry in NmF2. NmF2 is also characterized by two peaks namely pre-noon and post-noon peaks and noontime bite-out. The SSN is observed to have major effects on the variability of NmF2.

Keywords: NmF2, Solar activity, Equatorial ionosphere, Geomagnetic activity, Solar wind

1 Introduction

The ionosphere is an important part of the Earth's atmosphere, it plays a unique role in the Earth's environment because of strong coupling to regions below the ionosphere and above¹. The ionospheric F2-layer is primarily responsible for reflection of high frequency (HF) radiowaves in the ionosphere². Hence, knowledge of the ionospheric F2 peak density (NmF2), its peak height (hmF2), or the entire electron density profile $Ne(h)$, is of great significance for ionospheric forecasting and ionospheric propagation studies³. Also, NmF2 or its corresponding critical frequency (f_oF2) is an essential parameter as it determines the maximum usable frequency (MUF) for oblique radio waves propagation⁴. The ionospheric parameters exhibit significant diurnal, seasonal and solar cycle variations, etc., which results from changes in the solar EUV and X-ray, and from various chemical and dynamical processes in the Earth's atmosphere³. Studies on the variability of ionospheric parameters and climatology have been carried out by researchers^{1,5-11}.

Most of these works concentrated on stations outside equatorial latitudes region of African sector.

This may be due to shortage of sufficient data, because of earthof ionosonde stations in Africa especially West Africa. The purpose of this present paper is to investigate the climatology of NmF2 over Ouagadougou using ionosonde data and also to show the effects of solar and geomagnetic activity on NmF2.

2 Data and Method of Analysis

The data used for this study were obtained from ionograms recorded using ionosonde, IPS-42 located at Ouagadougou in Burkina Faso. Ouagadougou falls near the magnetic equator in the trough of the equatorial ionisation anomaly region in the African sector, (latitude 12.4°N, longitude 358.5°W, dip latitude +1.45). The period of study falls within solar cycles 21 and 22 (1976-1997). The geomagnetic activity, solar wind and solar activity data were taken from National Centers for Environmental Information (NOAA) formerly National Geophysical Data Resource Center (NGDC)¹² and National Space Science Data Centre (NSSDC)¹³. The solar activity index, SSN (solar sunspot number) data were also used to define the level of solar activity. The period of study was grouped into three using SSN. The year is considered high solar

*Corresponding author (E mail: k6abdul@yahoo.com)

activity (HSA), when the yearly average values of the $SSN > 100$, moderate solar activity (MSA), when $50 \leq SSN \leq 100$ and low solar activity (LSA) when $SSN < 50$ ⁴. The yearly average values of SSN in each of the levels of solar activity are shown in Table 1. In order to examine the effect of solar parameters and geomagnetic activity on $NmF2$, the solar wind, geomagnetic activity and solar activity indices used were disturbance storm time (Dst), interplanetary magnetic field (IMF), southward component of interplanetary magnetic field (Bz), solar wind speed (Vsw), solar wind dynamic pressure (Psw) and solar sunspot number (SSN). Since Dst is the measure of ring current, which is the indicator of geomagnetic storm at equatorial latitude regions. The authors also investigate the effect of geomagnetic activity on $NmF2$ ionosonde data using the geomagnetic activity index, Aa data. The $NmF2$ data were not separated into "quiet" and "disturbed" days, in order not to seriously reduce the quantity of usable ionospheric data. The Aa index data were used to explain the variability observed in the seasonal variations of $NmF2$. The Aa index data observed at the ground per day¹⁴. The geomagnetic activity may be divided into magnetic quiet days defined as days when $Aa < 20$ nT and magnetic disturbed days defined as days when $Aa \geq 20$ nT. The geomagnetic activity was also classified into four namely; quiet activity, recurrent activity, shock activity and fluctuating activity¹⁵⁻¹⁶.

The $F2$ -layer critical frequency (f_oF2) measured in MHz was obtained from Ouagadougou ionosonde data, and the peak electron density of $F2$ -layer ($NmF2$) measured in electron per metre cubic (el/m^3) was determined using the relation,

$$NmF2 = 1.24 \times 10^{10} (f_oF2)^2 (el/m^3) \quad \dots (1)$$

The daily mean hourly values of $NmF2$ for each hour for all the days of a month are referred to as the monthly mean hourly values for each of the months. These were obtained for all the months by averaging the hourly values of all the days of a month. The monthly mean hourly values of $NmF2$ were plotted against local time to examine diurnal variation for all the months of the year for the years considered. In order to examine the seasonal variations of $NmF2$, the months of the years were classified into different seasons based on the movement of the Sun as follows: March Equinox (March, April), June Solstice (May, June, July, August), September Equinox (September, October) and December Solstice (November, December, January, February).

The seasonal mean values were evaluated by finding the average of the monthly mean values under a particular season. In order to study the diurnal variation of seasonal mean hourly values, the year 1985 (LSA), the year 1993 (MSA) and 1991 (HSA) were selected to represent the years of low, moderate and high solar activities respectively. Finally, diurnal variations of annual mean hourly values of $NmF2$ are equally analysed. It is important to note that, there is no $NmF2$ data in months of July and August in 1997. These mean values of $NmF2$ were then correlated with geomagnetic and solar parameters i.e. annual average values of $Dst, IMF, Bz, Psw, Vsw, SSN$ in order to examine the how these parameters influence the variability of $NmF2$. The annual average values were used based on the fact that statistical studies have found that correlation on a daily or monthly basis is generally poor¹⁴. The correlation is much better on the basis of yearly averages.

3 Results and Discussion

3.1 Diurnal variation of $NmF2$

Figure 1 shows the diurnal variation of $NmF2$ during the years of HAS (1979-1982 and 1989-1991). $NmF2$ values are lowest around pre-sunrise hour (0500 LT), increase from the sunrise period (0600-0700 LT) attaining pre-noon peak around 1000-1100 LT and remain relatively high until after sunset around (1900 LT) where it begins to decrease. $NmF2$ is generally low in June solstice and high in equinoctial and December solstice months. The same trend of diurnal variation is observed during the years of MSA (1978, 1983, 1988 and 1992-1993) and years of LSA

Table 1 — of high, moderate and low solar activities.

High solar activity		Moderate solar activity		Low solar activity	
Years	SSN	Years	SSN	Years	SSN
1979	155.4	1978	92.5	1976	12.6
1980	154.6	1983	66.6	1977	27.5
1981	140.4	1988	100.2	1984	45.9
1982	115.9	1992	94.3	1985	17.9
1989	157.6	1993	54.6	1986	13.4
1990	142.6			1987	29.4
1991	145.7			1994	29.9
				1995	17.9
				1996	8.6
				1997	21.5

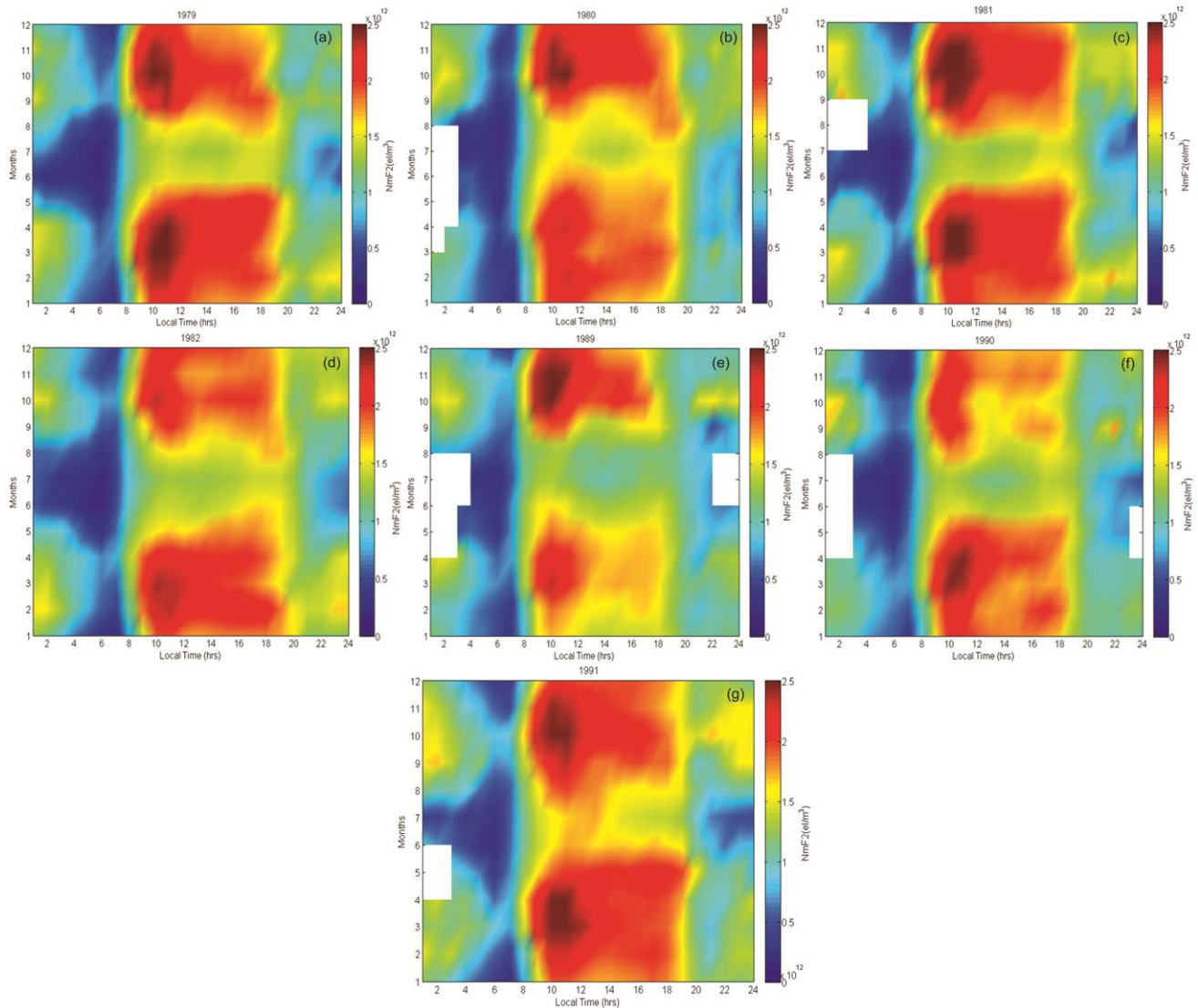


Fig. 1 — Diurnal variation of $NmF2$ over Ouagadougou, for years of high solar activity: (a) 1979, (b) 1980, (c) 1981, (d) 1982, (e) 1989, (f) 1990 and (g) 1991. (Blank white portion shows no data).

(1976-1977, 1984-1987 and 1994-1997) shown in Figs. 2 and 3. Diurnal variations in $NmF2$ during the years of HSA are highest, followed by the years of MSA and lowest at years of LSA. These results show that diurnal variations in $NmF2$ exhibits obvious seasonal and solar cycle dependence. Diurnal variations in $NmF2$ have been attributed to ionization and loss processes, dynamics of thermospheric neutral wind, 24-hour rotation of the earth about its axis¹⁸⁻¹⁹. It has also been suggested that diurnal variations may be due to geomagnetic and meteorological influences¹. The sunset increase in ionospheric values observed for the different solar activity conditions for low latitude due to the secondary fountain effect caused by the post-sunset

occurrence of a strong eastward electric field existing over the equatorial latitudes has been attributed²⁰.

3.2 Variations in seasonal mean of $NmF2$

Figure 4 shows seasonal mean of $NmF2$ variations during the years of HSA. Seasonal mean of $NmF2$ attains its maximum value in the equinoxes, followed by December solstice with the minimum values in June solstice for the years of HSA of 1979, 1981, 1989 and 1990. The trend is however different for the year 1980 and 1982. During 1980, seasonal mean in $NmF2$ is observed to be maximum in September equinox, followed by December solstice and then March equinox with minimum in June solstice while

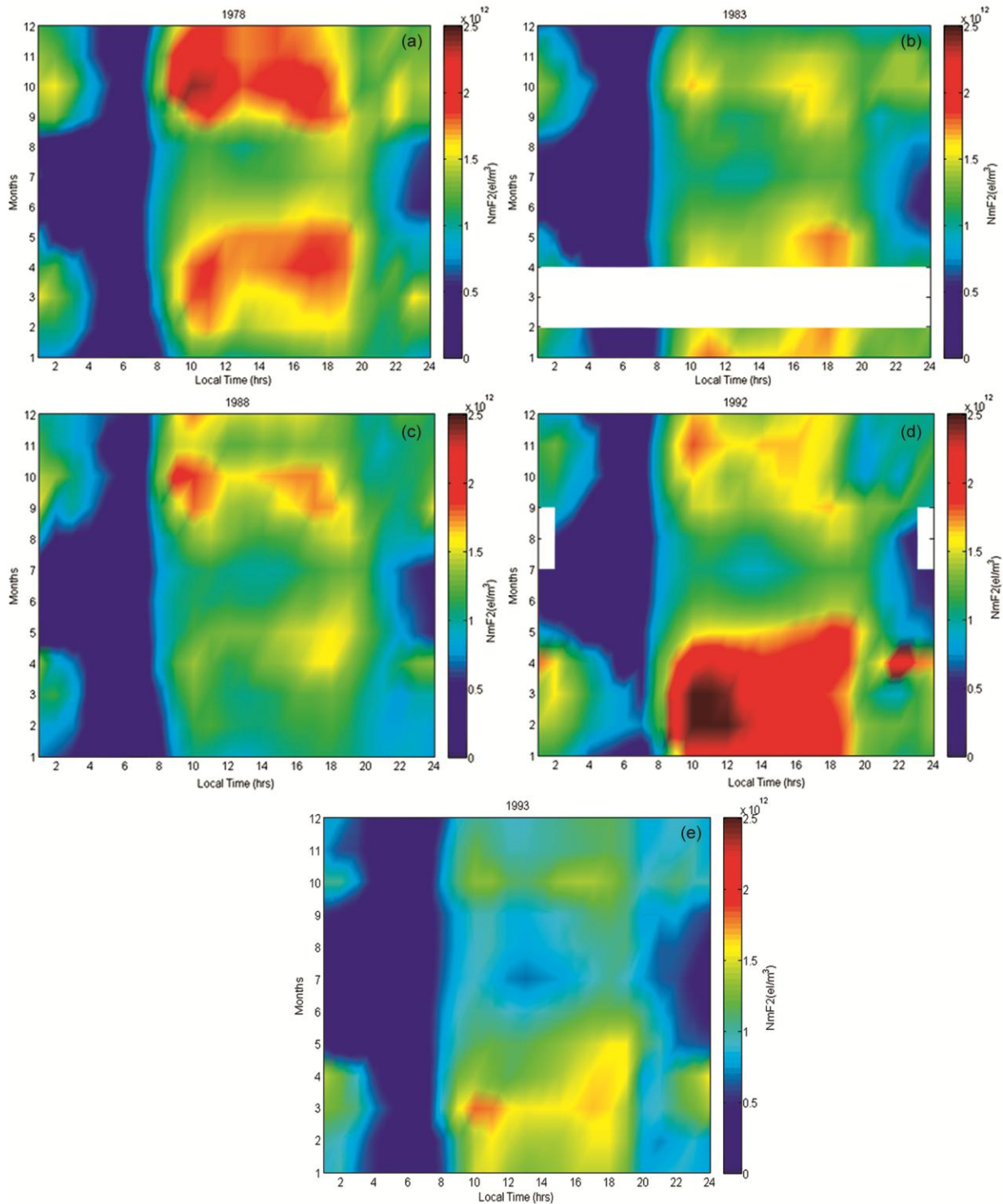


Fig. 2 — Diurnal variation of $NmF2$ over Ouagadougou, for years of moderate solar activity: (a) 1978, (b) 1983, (c) 1988, (d) 1992 and (e) 1993. (Blank white portion shows no data).

in 1982, the maximum values were observed in March equinox, followed by December solstice and then September equinox with the minimum values in June solstice. Thus generally, seasonal mean $NmF2$ is

maximum in March/September equinox and minimum in June solstice during the years of HSA. The seasonal mean variation of $NmF2$ during the years of MSA is shown in Fig. 5. The results show that it does follow

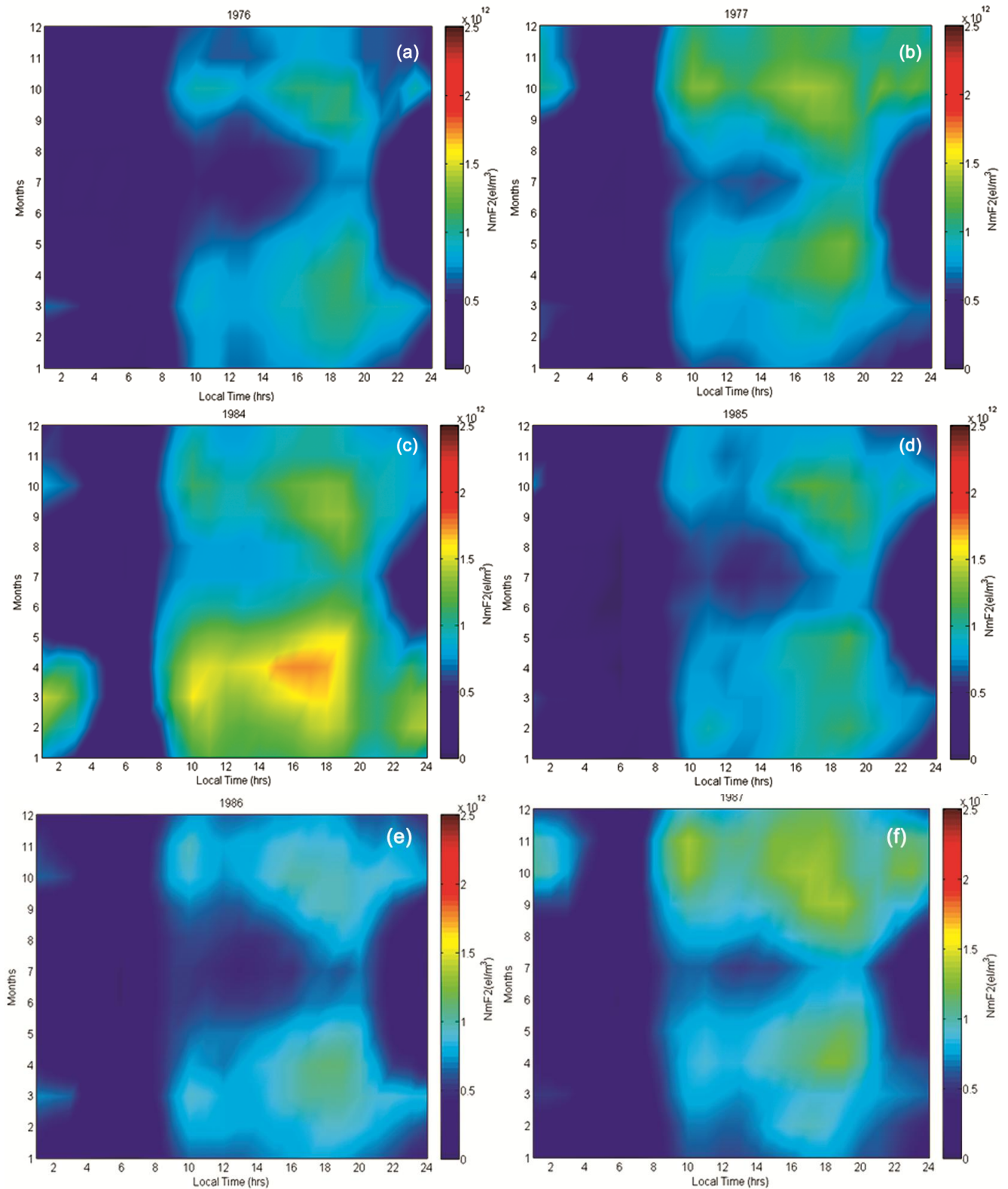


Fig. 3 — Diurnal variation of $NmF2$ over Ouagadougou, for years of low solar activity: (a) 1976, (b) 1977, (c) 1984, (d) 1987, (e) 1986 and (f) 1987. (Blank white portion shows no data). (*Contd.*)

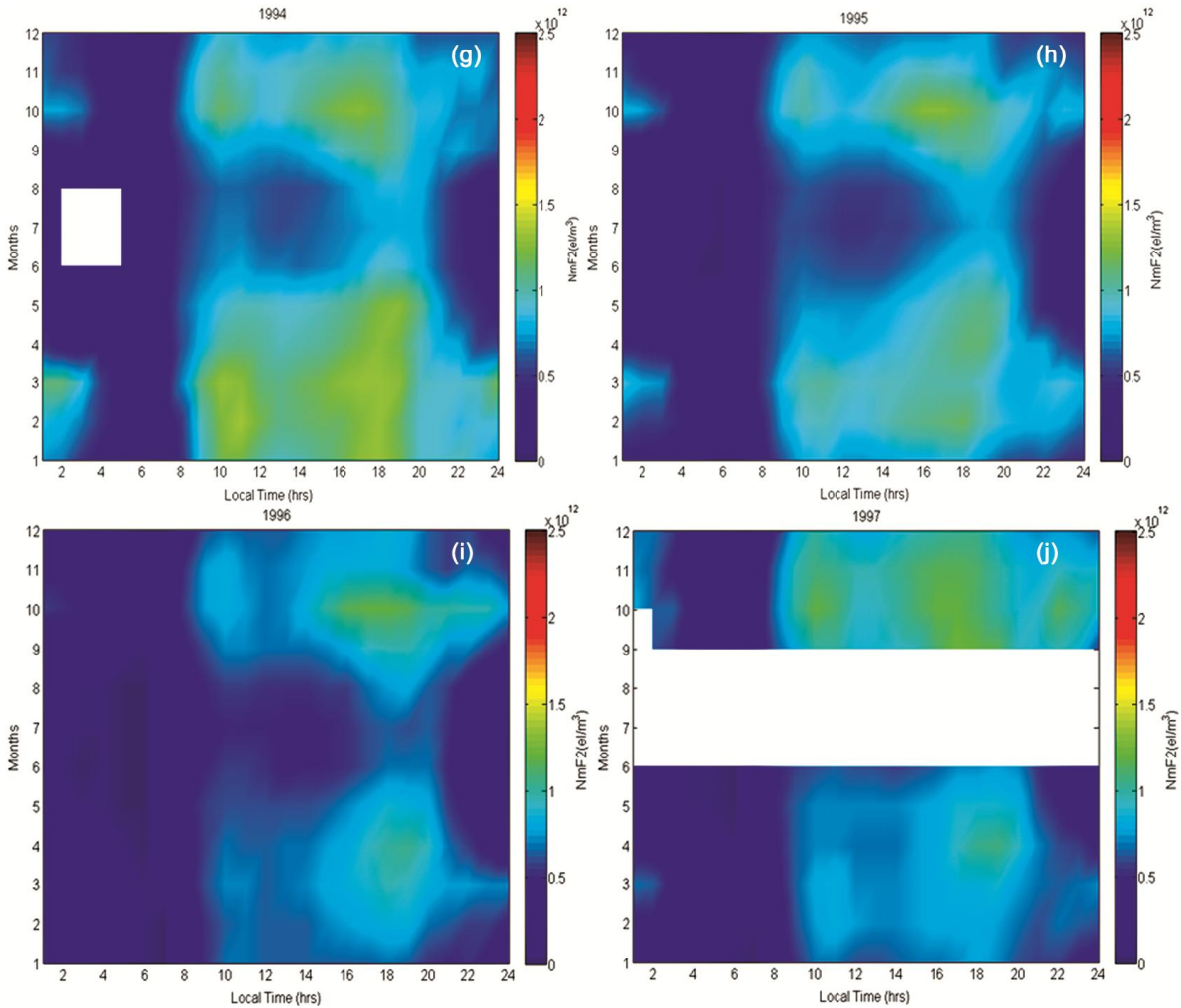


Fig. 3 — Diurnal variation of $NmF2$ over Ouagadougou, for years of low solar activity: (g) 1994, (h) 1995, (i) 1996 and (j) 1997. (Blank white portion shows no data).

similar trend or pattern as observed in the case of high solar activity periods. For instance, in 1978 the seasonal mean $NmF2$ attained maximum values in September equinox, followed by March equinox and then December solstice with the minimum values in June solstice while in 1983, maximum values of seasonal mean $NmF2$ are observed in March equinox, followed by September equinox and then December solstice with the lowest values in June solstice. In 1988, seasonal mean $NmF2$ recorded maximum values in September equinox, followed by December solstice and then March equinox with the minimum values in June solstice. During 1992 and 1993 maximum values are observed in March equinox, followed by December solstice and then September equinox with the lowest values in June solstice. Generally, seasonal mean $NmF2$ is maximum in March/September equinox and minimum in June

solstice during the years of MSA. The variations in the seasonal mean of $NmF2$ during the years of low solar activity are shown in Fig. 6. Seasonal mean $NmF2$ attained highest values in September equinox, followed by December solstice with the lowest values in June solstice except for 1984 and 1994 where maximum values are observed in March equinox rather than September equinox. Variations in the seasonal mean of $NmF2$ therefore exhibit solar cycle dependence, being highest during the years of high solar activity, followed by the years of moderate solar activity and minimum during the years of low solar activity. These results further confirm some of the characteristics attributes of equatorial ionosphere such as semi-annual variation, December (winter) anomaly, equinoctial asymmetry etc. as documented in literature²¹⁻²².

Figures 4, 5 and 6 show that seasonal mean of $NmF2$ demonstrates semi-annual variation, having

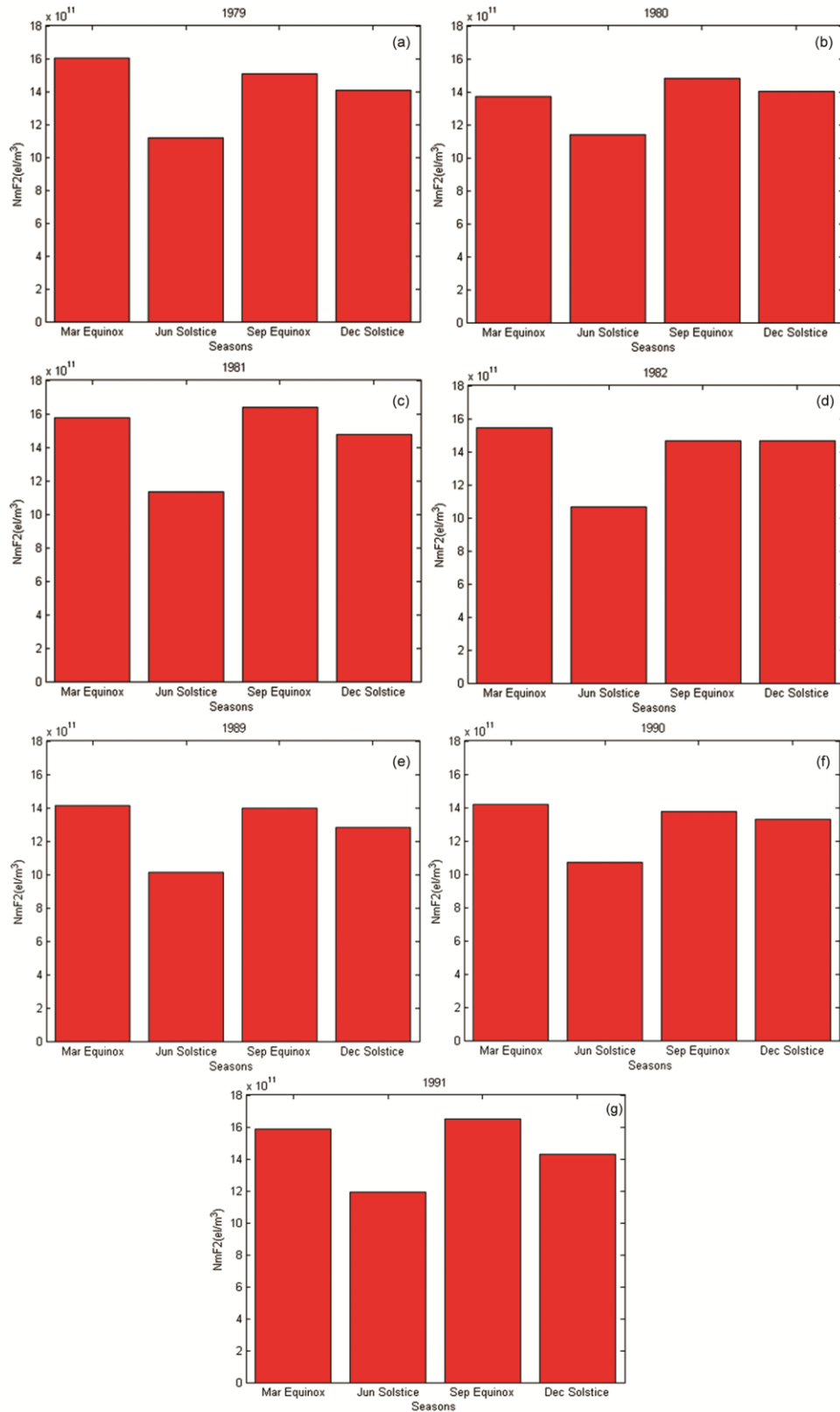


Fig. 4 — Seasonal variation of $NmF2$ over Ouagadougou, for years of high solar activity: (a) 1979, (b) 1980, (c) 1981, (d) 1982, (e) 1989, (f) 1990 and (g) 1991. (Blank white portion shows no data).

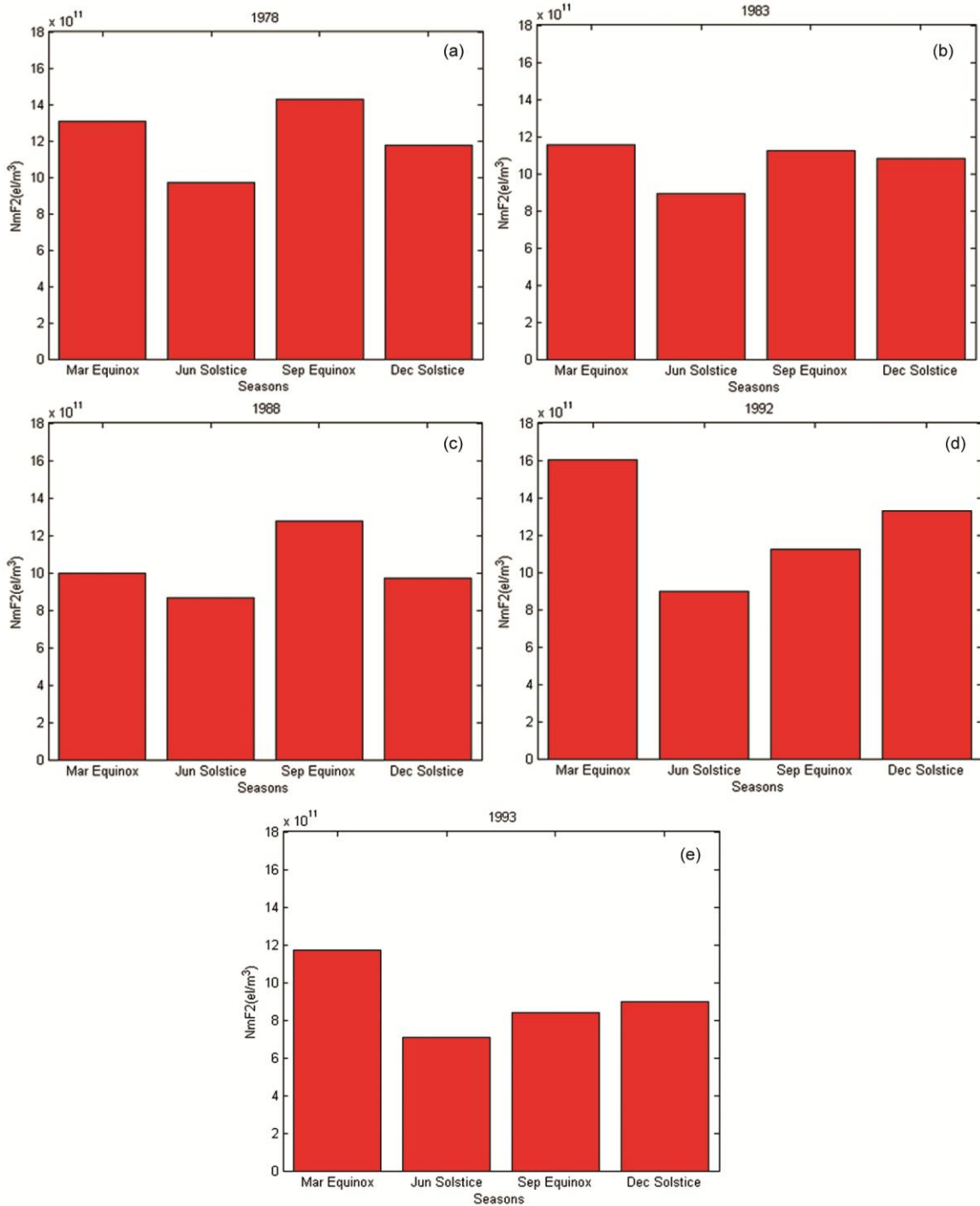


Fig. 5 —Seasonal variation of $NmF2$ over Ouagadougou, for years of moderate solar activity: (a) 1978, (b) 1983, (c) 1988, (d) 1992 and (e) 1993. (Blank white portion shows no data).

higher values in equinoxes than solstices. Also, the values during December (winter) solstice are observed to be greater than those of June (summer) solstice. The results further revealed the equinoctial asymmetrical characteristics of $NmF2$ in the equatorial regions. In addition to the varying Sun-

earth distance due to the earth's elliptic orbit, variations in the seasonal mean of $NmF2$ have been attributed to factors such as thermospheric wind, neutral wind and dynamo electric field which in itself exhibit seasonal variations. The seasonal variation of $NmF2$ was also attributed to the combined effects of

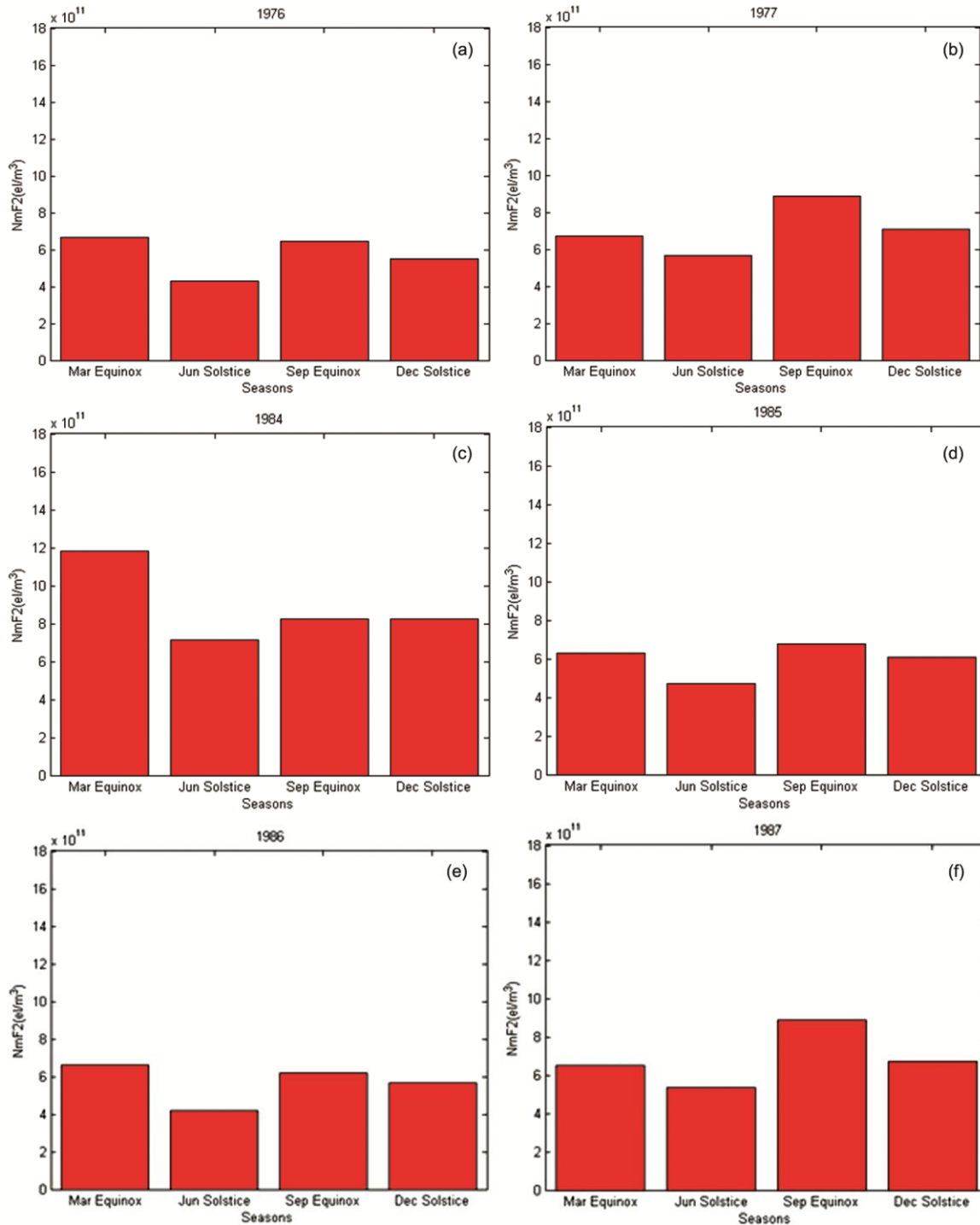


Fig. 6 —Seasonal variation of $NmF2$ over Ouagadougou, for years of low solar activity: (a)1976, (b) 1977, (c) 1984, (d) 1985, (e) 1986 and (f) 1987. (Blank white portion shows no data). (Contd.).

changes in atmospheric composition $[O]/[N_2]$ and photo-ionization production rates which is being controlled by solar zenith²³⁻²⁴.

The significant semi-annual anomaly (variation) withpeak at the equinoxes and smallest at the solstices

observed in this study is in conformity with previous studies^{20,25-30}. The variation of the diurnal tide in the lower thermosphere as a possible mechanism capable of inducing the semi-annual variation of the low latitude $NmF2$ was proposed²⁹. The semi-annual

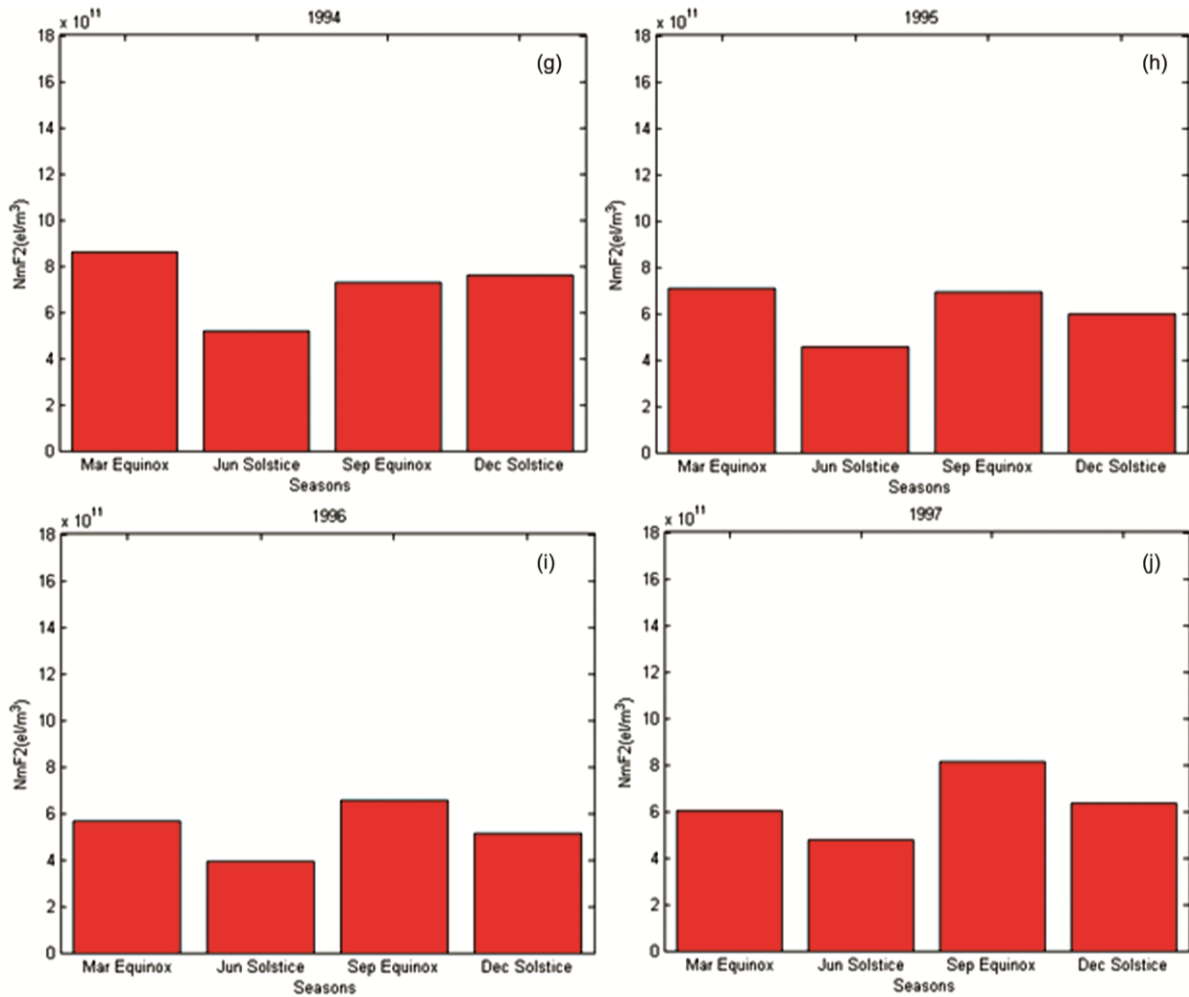


Fig. 6 — Seasonal variation of $NmF2$ over Ouagadougou, for years of low solar activity: (g)1994, (h) 1995, (i) 1996 and (j) 1997. (Blank white portion shows no data).

anomaly in $foF2$ associated to the semi-annual variation of the upper atmosphere temperature was proposed³⁰. Also, the semi-annual anomaly observed in $NmF2$ which was due to semi-annual variation in neutral densities linked with geomagnetic and auroral activities was suggested by Torr *et al.*³¹. The seasonal anomaly observed in this study had earlier been observed at low latitude stations³²⁻³⁴ and recently it has been highlighted^{4,7,22,27-28,35}. This anomaly is credited to seasonal change of O/N_2 (density of ratio of atom oxygen to molecule nitrogen) concentration^{7,21}, variations in the Sun-Earth distance³², changes in temperature³⁶, interhemispheric transport of ionization³⁷, and the upward energy flux³⁸. $NmF2$ show annual or non-seasonal anomaly in which the December values are greater than June values²⁸. A possible cause of the non-seasonal anomaly is the changes in Sun-Earth distance^{28,39}. Equinoctial

asymmetry observed in this work has been previously observed^{4,40-45} for equatorial and low latitudes. This observation has been credited to a combination of numerous factors such as equatorial vertical plasma drift, thermospheric composition or neutral density⁴⁵. The anomalous behaviour of $NmF2$ observed in some years where $NmF2$ values are higher at December solstice months than either March/September equinox can be attributed to the effect of geomagnetic activity. Those months are magnetically disturbed months. The higher values of Aa and Dst indices are indicators of geomagnetic activity and geomagnetic storm. The months affected during December solstices and the years are shown in Table 2.

3.3 Seasonal Mean Diurnal Variation of $NmF2$

Figures 7, 8 and 9 show mean diurnal plots of $NmF2$ for all the seasons of the years during low, moderate and high solar activities respectively. During

the year of low solar activity, $NmF2$ follows the same diurnal trend throughout the day for all the seasons. $NmF2$ generally increases from a pre-sunrise minimum, attains pre-noon peak and post sunset peak. The pre-sunrise minimum and the post sunset maximum tend to exhibit seasonal differences. For the equinox months the pre sunrise minimum is observed around 0600 LT while the post sun-set maximum occurs around 1800LT. However for the solstices, the pre sunrise minimum is observed value at 0700 LT while the post-sunset peak is observed around 1900LT. The pre-noon peak is observed around 1000LT irrespective of the season (see Fig. 9). These two peaks border the noontime “bite-out” which occur around 1300 LT. There is sharp drop in

$NmF2$ after sunset till pre-sunrise at 0600 LT. The post-noon peak is greater than pre-noon peak. The pattern of variation is repeated during both moderate and high solar activities periods. Figure 8 shows that during moderate solar activity periods $NmF2$ increases from the pre-sunrise minimum around 0600-0700 LT and reaches the pre-noon peak at 1000 LT. The post-noon peak occurs at 1800 LT for all seasons and noon-bite also occurs at 1300 LT except December solstice where it occurs at 1200 LT. Thereafter $NmF2$ increases further till it attains post-sunset minimum value at 2000 LT except for June solstice that doesn't exhibit the post-sunset minimum. $NmF2$ values are higher at equinoxes than at solstices except at night time around after 2300 LT up to around sunrise period (0600 LT) where December solstice is higher than September equinox. It is however worthy of note that $NmF2$ during March equinox is extremely higher than that of September equinox. Figure 9 shows the plot of seasonal diurnal mean values of $NmF2$ during the year of high solar activity. As expected, seasonal diurnal means during HSA are higher in magnitude than those of years of MSA and LSA. $NmF2$ rises from the pre-sunrise minimum between 0600 LT and 0700 LT and reaches the pre-noon peak around 1000 LT. A post-noon peak occurs around 1700 LT and it decreases afterward till the post-sunset minimum is observed between 2000 LT

Table 2 — Maximum values of geomagnetic indices during years with anomalous variation in seasonal mean $NmF2$.

Years	Geomagnetic Indices	
	Aa	Dst
1977	21	-22
1980	24	-20
1982	49	-50
1984	29	-21
1987	22	-23
1988	27	-30
1992	37	-54
1993	31	-24
1994	40	-40
1997	21	-23

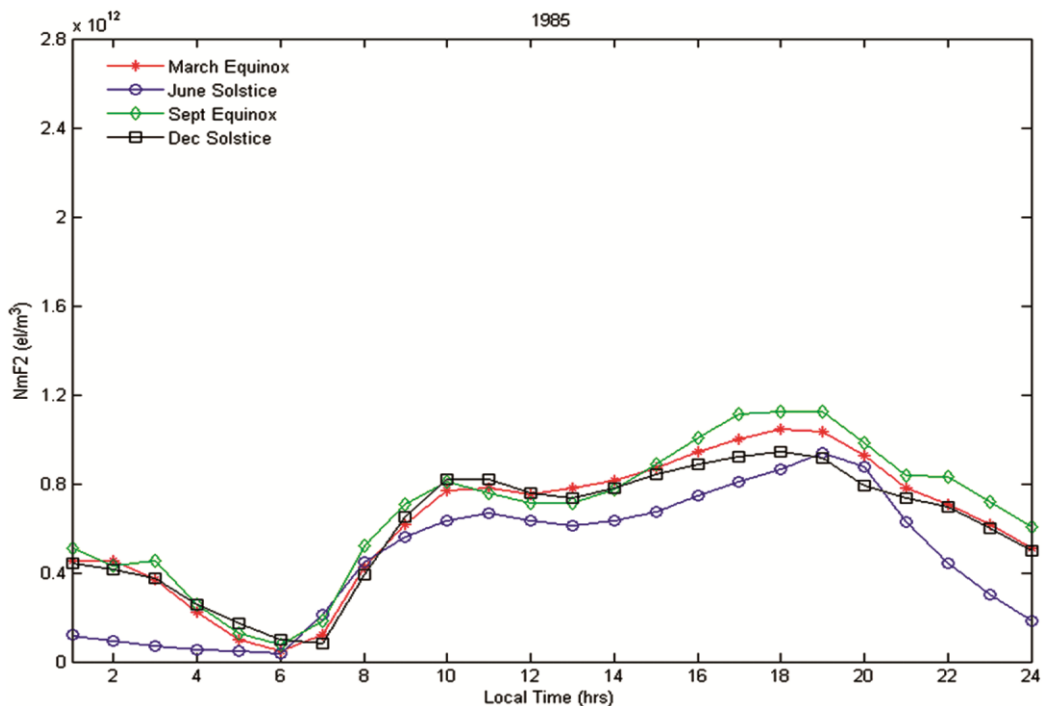


Fig. 7 — Diurnal variation of $NmF2$ for all seasons over Ouagadougou at low solar activity year (1985).

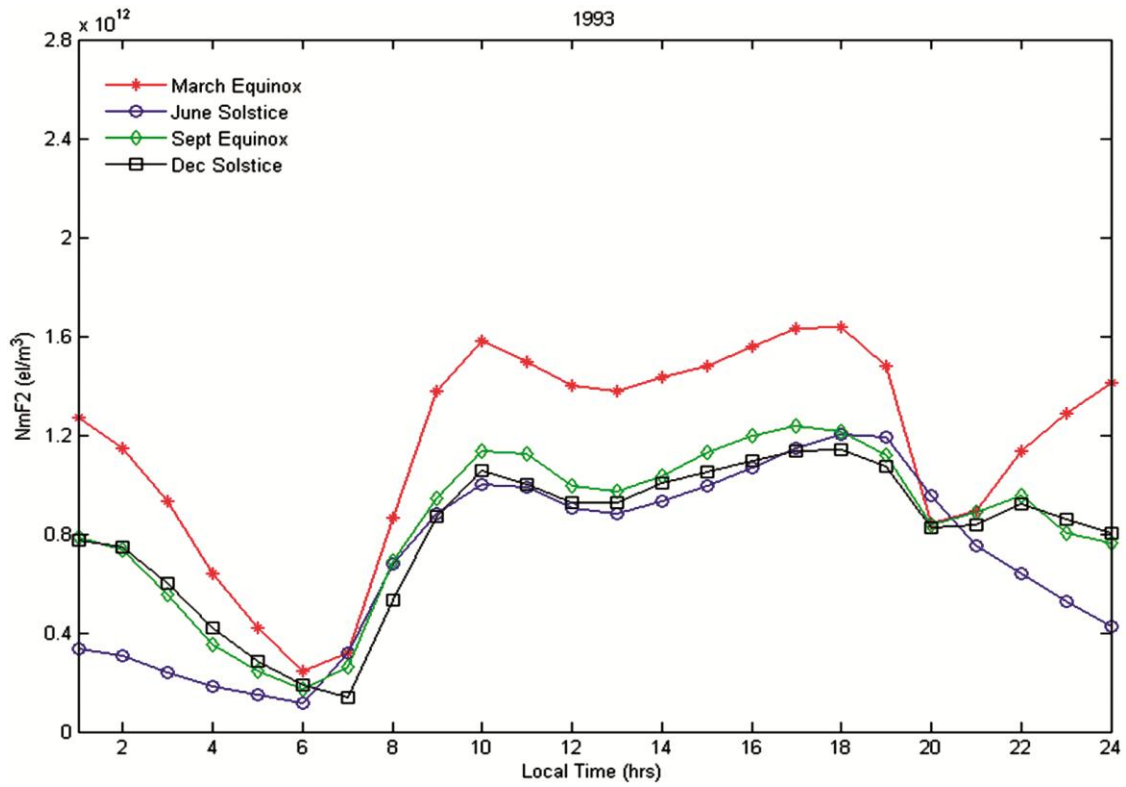


Fig. 8 — Diurnal variation of $NmF2$ for all seasons over Ouagadougou at moderate solar activity year (1993).

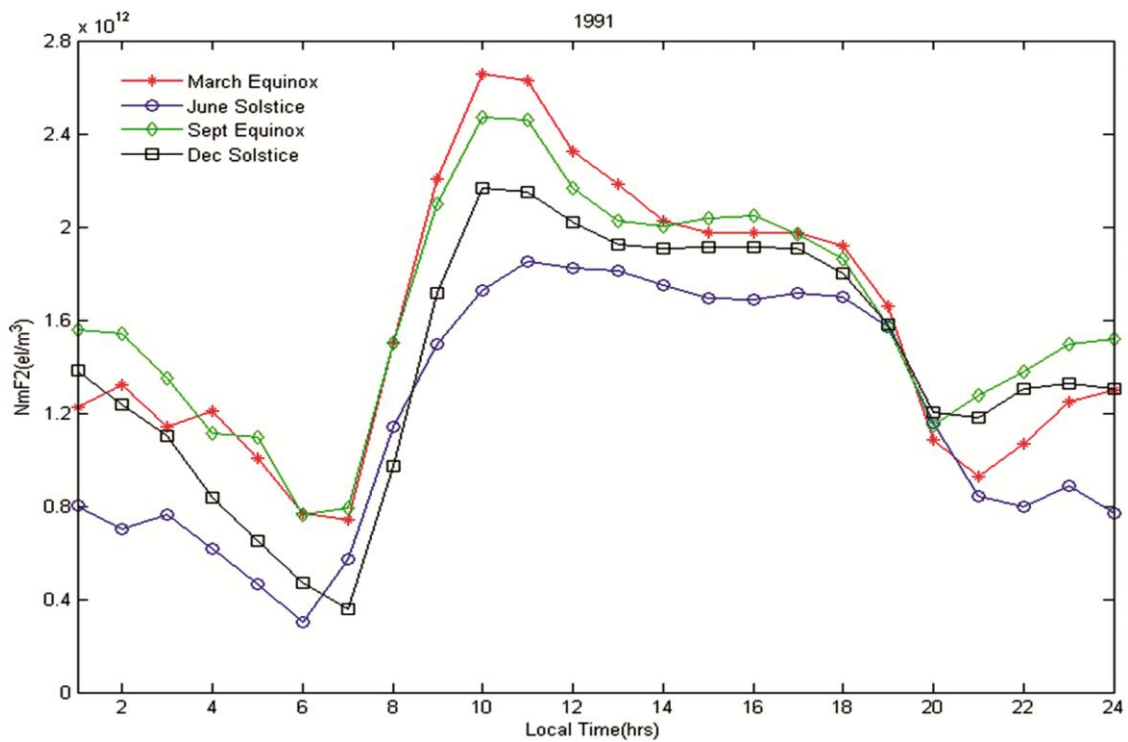


Fig. 9 — Diurnal variation of $NmF2$ for all seasons over Ouagadougou at high solar activity year (1991).

and 2200 LT at all seasons and there is rapid rise in $NmF2$ after the post-sunset minimum. Also, there is noon bite-out which is not well pronounced at solstices and it occurs mostly around 1400 LT. $NmF2$ is higher at equinoxes than the solstices and the March equinox is greater than the September equinox especially during the daytime. A remarkable difference between the diurnal profiles of $NmF2$ during HSA is that the pre-noon peak is greater than the post-noon peak.

Figure 10 illustrates the diurnal variation of $NmF2$ on an annual basis for the years of low, moderate and high solar activities. The same diurnal trends were observed in $NmF2$ and its dependence on solar activity is obviously seen, that is, $NmF2$ values during HSA year are highest, followed by the year of MSA and minimum during the year of LSA. The pre-noon peak which is higher than the post-noon peak for year of high solar activity and the reverse is for the year of low solar activity seen in seasonal mean values is also clearly observed, but $NmF2$ is almost symmetry during the year of moderate solar activity. The results obtained clearly show that June solstice maintained the minimum mean $NmF2$ values most of the time. These results agree with the fact that $NmF2$ values at equatorial/low latitude stations are larger during equinox months than solstice months, since the solar zenith angle is lowest during the equinoxes. Also, during the equinoxes the atmosphere is observed

to be colder and denser therefore the ionosphere will tend to move closer to the Earth thereby rise the electron density at equatorial ionosphere. The peculiar features observed in the variation of peak electron density of the equatorial ionosphere like pre-noon peak, post-noon peak, noontime bite-out and post-sunset minimum observed in the electron density values have been explained in term of winds and the $E \times B$ force effect on the plasma⁴⁶⁻⁵¹. In the equatorial region, the electric field E in combination with the earth's magnetic field B yields the $E \times B$ force that causes vertical drift of ionization¹⁰. The direction of $E \times B$ force is upward throughout the daytime and downward during the nighttime and thus there is upward drift of plasma in the daytime and downward drift of plasma in the night time. It was revealed that the occurrence of a sharp increase of the upward velocity in the dusk sector just before it reverses to its downward direction is the main attribute of the equatorial F region vertical drift. The evening upward velocity enhancement is accountable for the speedy rise of the F layer after sunset⁵².

3.4 Variation of $NmF2$ with solar and geomagnetic activity indices

Figure 11 shows the time series plots of solar parameters and geomagnetic activity index along with $NmF2$ during the solar cycles 21 and 22. The solar cycle variations of $NmF2$ are quite obvious as its

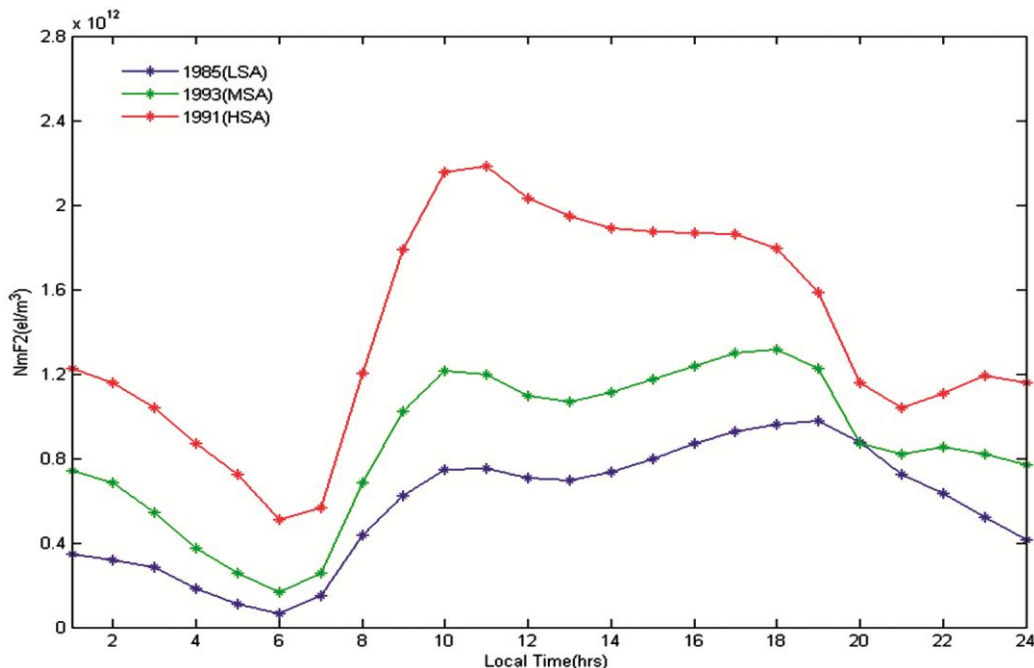


Fig. 10 — Diurnal variation of annual mean of $NmF2$ over Ouagadougou for years of low, moderate and high solar activities.

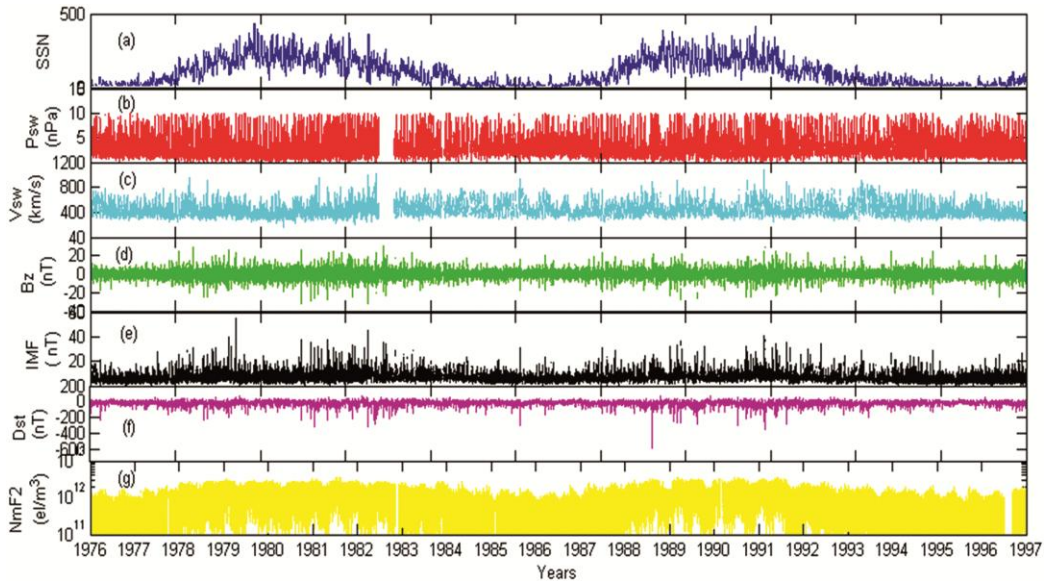


Fig. 11 — Time variation (hourly values) of various solar, geomagnetic and ionospheric indices, panels (a) *SSN* (b) *Psw* (nPa), (c) *Vsw* (km/s), (d) *Bz* (nT), (e) *IMF* (nT), (f) *Dst* (nT) and (g) *NmF2* (el/m³) during solar cycles 21 and 22.

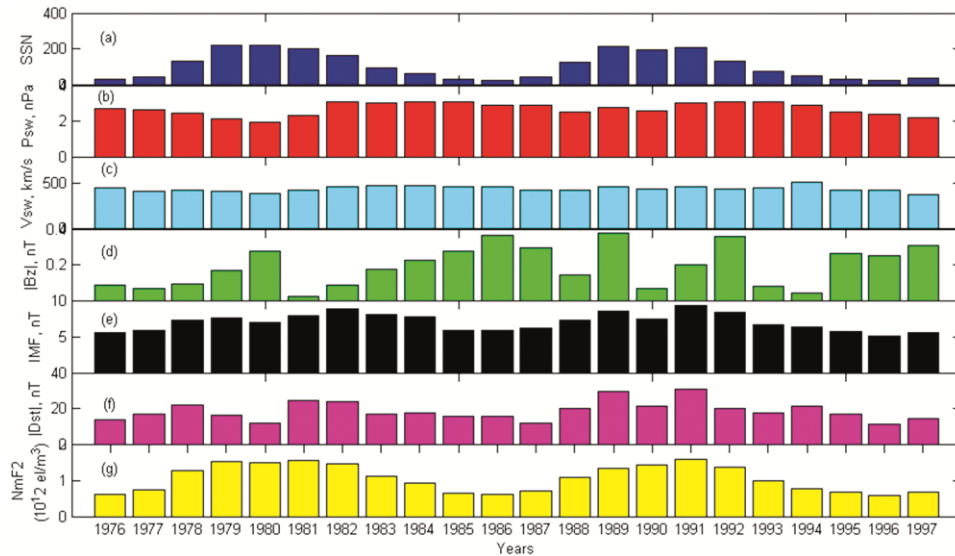


Fig. 12 — Yearly variation of solar, geomagnetic and ionospheric indices; panels (a) *SSN*, (b) *Psw* (nPa), (c) *Vsw* (km/s) (d) *Bz*/(nT), (e) *IMF* (nT), (f) *Dst* /(nT) and (g) *NmF2* (10¹²el/m³) during solar cycles 21 and 22.

variation pattern follows the same trend with *SSN* for the two cycles. The case is however different for solar wind indices and geomagnetic activity index. These results have earlier been reported by Ouattarra *et al.*⁴. In order to further look at the influence of the solar and geomagnetic activity indices in the variability of *NmF2*, the yearly average values of the solar activity, solar wind and geomagnetic activity indices along with *NmF2* during the period of study are shown in Fig. 12. It was observed that the solar cycle variations

of *IMF* and *NmF2* are apparent as its variation pattern also follows the same trend with *SSN*. Hence, *NmF2* and *IMF* follow 11 years solar cycle variation as their behaviour changes each 11-years. One of the reasons why *NmF2* and *IMF* show solar cycle influence may be because of the fact that F-region electron density (*NmF2*) is primarily produced by solar radiation (particularly EUV and X ray)¹⁹, while *IMF* is the Sun's magnetic field which emanated from the Sun. Although solar wind and geomagnetic activity

indices display solar cycle response, their effects on $NmF2$ are not quite obvious except IMF that shows clear solar cycle effect.

In order to ascertain their level of influence on the variability of $NmF2$, annual mean values of $NmF2$ were correlated with each of the indices for the entire period under study. $NmF2$ versus Dst , $NmF2$ versus Psw , $NmF2$ versus Bz , $NmF2$ versus IMF ,

$NmF2$ versus Vsw and $NmF2$ versus SSN respectively are shown in Fig. 13. The straight lines of best fit is given by the linear regression. The degrees of correlation are also indicated. The statistical result is as shown in Table 3. $NmF2$ shows the highest value of correlation coefficient with SSN , with the correlation coefficient (R) of 0.967 and the coefficient of determination (R^2) of 0.936 which

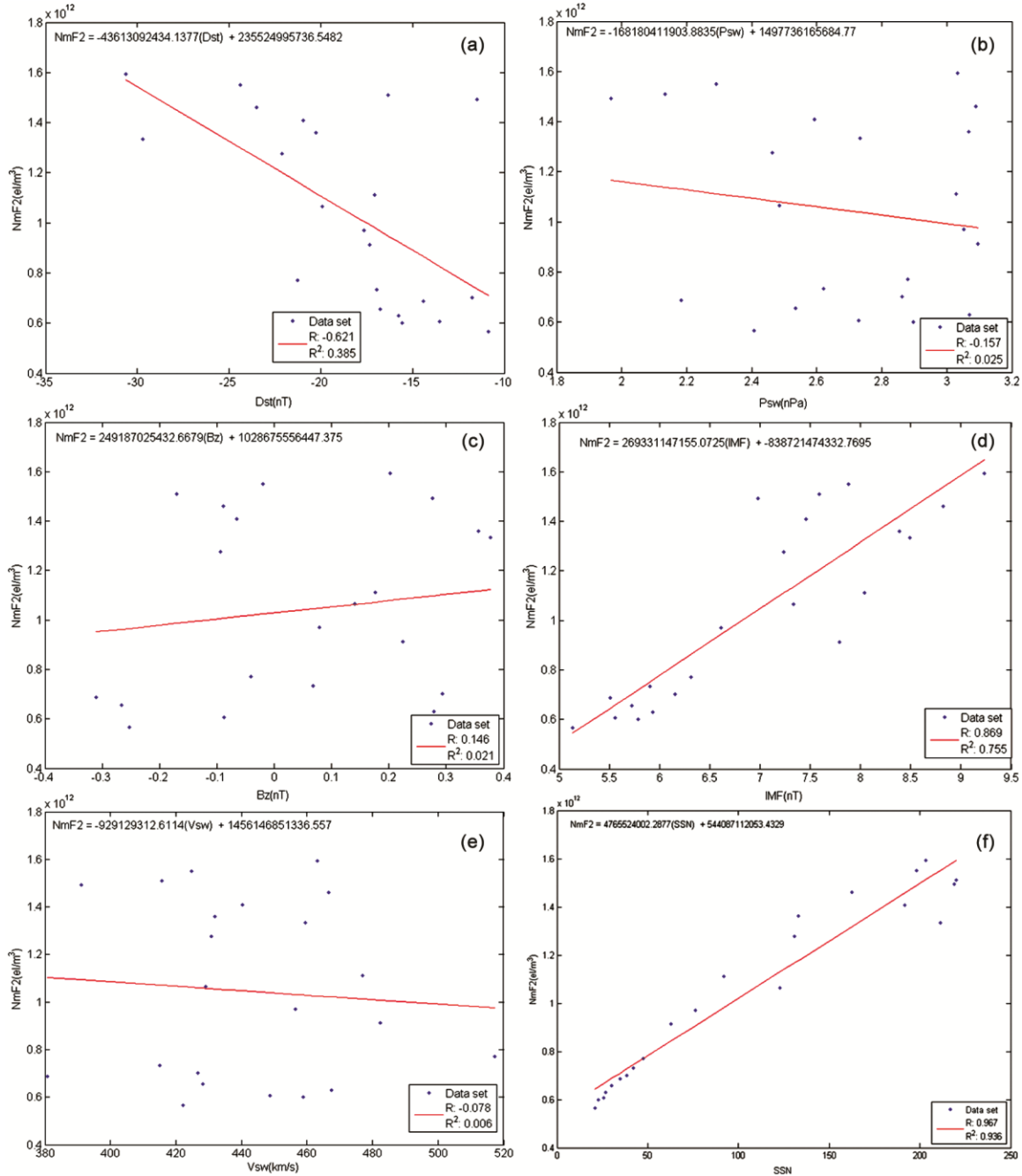


Fig. 13 — The scatter plot of annual average values for (a) $NmF2$ versus Dst , (b) $NmF2$ versus Psw , (c) $NmF2$ versus Bz , (d) $NmF2$ versus IMF , (e) $NmF2$ versus Vsw and (f) $NmF2$ versus SSN for the interval of 1976-1997

Table 3 — Correlation coefficient (R), coefficient of determination (R^2) and linear regression coefficients - (Intercept (a) and slope (b)) between $NmF2$ and geomagnetic and solar indices.

Indices	R	R^2	a	b
Dst (nT)	-0.621	0.385	2.355×10^{11}	4.361×10^{10}
Psw (nPa)	-0.157	0.025	1.498×10^{12}	-1.682×10^{11}
Bz (nT)	0.146	0.021	1.029×10^{12}	2.492×10^{11}
IMF (nT)	0.869	0.755	-8.387×10^{11}	2.693×10^{11}
Vsw (km/s)	-0.078	0.006	1.456×10^{12}	-9.291×10^8
SSN	0.967	0.936	5.441×10^{12}	4.766×10^{10}

means that 93.6% of $NmF2$ can be accounted for using SSN and followed by IMF with the correlation coefficient (R) of 0.869 and the coefficient of determination of 0.755 which implies 75.5% of the total variation in $NmF2$ can be explained by the linear relationship between $NmF2$ and IMF . The correlation coefficient (R) of $NmF2$ versus Dst is -0.621, though anti-correlated. The coefficient of determination is 0.385 which means 38.5% of the total variation in $NmF2$ can be explained by the linear relationship between $NmF2$ and Dst . The coefficient of determination (R^2) of $NmF2$ against Psw is 0.025 which implies that 2.5% of $NmF2$ can be accounted for using Psw . The coefficient of determination of $NmF2$ versus Vsw is 0.006 which means that only 0.6% of $NmF2$ can be accounted for using Vsw . Finally, the coefficient of determination (R^2) of $NmF2$ against Bz is 0.021 indicates that only 2.1% of $NmF2$ can be explained using Bz . Generally, the correlation between $NmF2$ and SSN and IMF respectively is very high and positive, but that of $NmF2$ against Dst is high and negative. Also, the correlation between $NmF2$ and Psw and Vsw respectively is very low and negative. The results show solar sunspot number (SSN) which stands as solar activity proxy, followed by the interplanetary magnetic field, (IMF) and then the disturbance storm time, (Dst), have major effects on the peak electron density of $F2$ -layer, ($NmF2$).

4 Conclusion

The variability of $NmF2$ and the effect of the solar and geomagnetic activity on $NmF2$ was studied. $NmF2$ shows both diurnal and seasonal dependence. It implies that equatorial ionosphere is not a stable membrane during the day. The seasonal mean of $NmF2$ displays semi-annual, winter and annual anomalies. $NmF2$ is maximum in March/September equinox and minimum in June solstice at all levels of solar activities. $NmF2$ also shows equinoctial

asymmetries which indicate there are differences between March and September equinoctial peak. $NmF2$ exhibits solar cycle effect. $NmF2$ values are highest at years of HSA, followed by the years of MSA and LSA respectively. Diurnal variation of seasonal mean values of $NmF2$ is characterized by two peaks namely pre-noon and post-noon peaks and noontime bite-out at all levels of solar activity. The post-noon peak is greater than pre-noon peak at year of low solar activity while reverse is the case at year of high solar activity. The correlation of $NmF2$ with the solar and geomagnetic activity indices revealed that SSN , followed by IMF and then Dst have major effects on $NmF2$.

Acknowledgements

The authors are grateful to the host of the ionosonde equipment in Ouagadougou and the Centre National d'Etude de Telecommunication (CNET) France, for making the ionosonde data at Ouagadougou available for scientific work. The authors are also grateful to the National Center for Environmental Information (NAOO) and National Space Science Data Centre (NSSDC) for the use of solar activity, solar wind and geomagnetic activity data.

References

- 1 Rishbeth H & Mendillo M, J Atmos and Sol-Terr Phys, 63 (2001) 1661.
- 2 Hoque M M & Jakowski N, Ann Geophys, 30(5) (2012) 797.
- 3 Lei J, Liu L, Wan W & Zhang S R, Radio Sci, 40 (2) (2005) 1.
- 4 Ouattara F, Amory-Mazaudier C, Fleury R, Lassudrie Duchesne P, Vila P & Petitdidier M, Ann Geophys, 27 (2009) 2503.
- 5 Kawamura S, Balan N, Otsuka Y & Fukao S, J Geophys Res, 107 (2002) 1166.
- 6 Unnikrishnan K, Nair R B & Venugopal C, J Atmos Sol-Terr Phys, 64 (2002) 1833.
- 7 Zhang S R, Holt J M, Anthony P, Eyken V, McCready M, Amory-Mazaudier C, Fukao S & Sulzer M, Geophys Res Lett, 32 (2005) L20102.
- 8 Adeniyi J O, Oladipo O A & Radicella S M, J Atmos Sol-Terr Phys, 69 (2007) 721.

- 9 Zhao B, Wan W, Liu L & Ren Z, *Ann Geophys*, 27 (2009) 3861.
- 10 Oladipo O A, Adeniyi J O, Radicella S M & Adimula, I A, *Adv Space Res*, 47 (2011) 496.
- 11 Chauhan V, Singh O P & Birbal S, *J Radio Space Phys*, 40 (2011) 26.
- 12 <http://www.spidr.ngdc.noaa.gov/spidrand>
- 13 <http://www.omniweb.com>
- 14 <http://isgi.latmos.ipsl.fr/>
- 15 Legrand J P & Simon P A, *Ann Geophys*, 7 (1989) 565.
- 16 Ouattara F & Amory-Mazaudier C, *J Atmos Sol-Terr Phys*, 71 (2009) 1736.
- 17 Klobuchar J A & Doherty P H, The correlation of daily solar flux values with total electron content, in M-C. Lee (ed.), *Proceedings of the international Beacon Satellite Symposium*, Cambridge, Massachusetts, Plasma Fusion Center, Massachusetts Institute of Technology, USA, (1992)192.
- 18 Bremer J, *Adv Radio Sci*, 2 (2004) 253.
- 19 Motoba T, 56(1-4) (2009) 447.
- 20 Bhuyan P K, Lakha Singh & Tyagi T R, *Ann Geophys*, 4 (1986) 131.
- 21 Rishbeth H & Garriot O K, *Introduction to ionospheric Physics*, (Academic press, New York), (1969).
- 22 Rishbeth H, Muller-Wodarg I C F, Zou L, Fuller-Rowell T J, Millward G H, Moffett R J, Idenden D W & Aylward A D, *Ann Geophys*,18 (2000) 945.
- 23 Liu L, Wan W, Chen Y, Le H & Zhao B, *Chin J Space Sci*, 32(5) (2012) 665.
- 24 Mayr H G & Mahajan K K, *J Geophys Res*, 76 (4) (1971) 1017.
- 25 Chaman L, *J Atmos Sol-Terr Phys*, 57 (1) (1995) 45.
- 26 Huang Y-N & Cheng K, *J Geophys Res*, 101 (1996) 24513.
- 27 Araujo-Pradere E A, *Rev Bras Geof*, 15(2) (1997) 161.
- 28 Zou L, Rishbeth H, Muller-Wodarg I C F, Aylward A D, Millward G H, Fuller-Rowell T J, Idenden D W & Moffett R J, *Ann Geophys*, 18 (2000) 927.
- 29 Ma R, Xu J & Liao H, *J Atmos Sol-Terr Phys*, 65 (2003) 47.
- 30 Yonezawa T, *J Atmos Sol-Terr Phys*, 33 (1971) 889.
- 31 Torr M R & Torr D G, *J Atmos Sol-Terr Phys*, 35 (1973) 2237.
- 32 Yonezawa T, *J Radio Res Laboratories*, 6 (1959) 651.
- 33 Croom S A, Robbins A R & Thomas J O, *Nature*, 185 (1960) 902.
- 34 Jacchia L G, *Rev Mod Phys*,35 (1963) 973.
- 35 Millward G H, Rishbeth H, Fuller-Rowell T J, Aylward A D, Quegan S & Moffert R J, *J Geophys Res*, 101 (A3) (1996) 5149.
- 36 Appleton E V & Barnett M A F, *Proc R Soc*, 113 (1926) 450.
- 37 Rothwell P, Diffusion of ions between F layers at magnetic conjugate points in *Proc. International Conference on the Ionosphere*, Institute of Physics and Physical Society, London, (1963) 217.
- 38 Madea K, Hedin AE & Mayr H G, *J Geophys Res*, 91 (1992) 4461.
- 39 Buonsanto M J, *South Pacific J Natural Sci*, 8 (1986) 58.
- 40 Essex E A, *J Atmos Sol-Terr Phys*, 39 (1977) 645.
- 41 Balan N, Otsuka Y, Bailey G J & Fukao S, *Geophys Res let*, 24 (1997) 2287.
- 42 Balan N, Otsuka Y, Bailey G J & Fukao S, *J Geophys Res*, 103 (1998) 9481.
- 43 Bailey G J, Su Y Z & Oyama K -I, *Ann Geophys*, 18 (2000) 789.
- 44 Chen Y, Liu L, Wan W, Yue X & Su S -Y, *J Geophys Res*, 114 (2009) A08306.
- 45 Chen Y, Liu L, Wan W & Ren Z, *Ann Geophys*, 30 (2012) 613.
- 46 Rajaram G & Rastogi R G, *J Atmos Sol-Terr Phys*, 39 (1977) 1175.
- 47 Radicella S M & Adeniyi J O, *Radio Sci*, 34 (5) (1999) 1153.
- 48 Lee C C & Reinisch B W, *J Atmos Sol-Terr Phys*, 68 (2006) 2138.
- 49 Lee C C, Reinisch B W, Su S Y & Chen W S, *J Atmos Sol-Terr Phys*, 70 (2008) 184.
- 50 Liu H & Watanabe S, *J Geophys Res*, 113 (2008) A0831.
- 51 Ogwala A, Somoye E O, Onori E O & Adeniji-Adele R A, *Physics J*, 1(2) (2015) 137.
- 52 Fejer B G, de Paula E R, Gonzalez SA & Woodman R F, *J Geophys Res*, 96(8) (1991) 901.